Available online at www.sciencedirect.com

SCIENCE DIRECT®

Journal of Biomedical Informatics 37 (2004) 10–18

Journal of Biomedical Informatics

www.elsevier.com/locate/yjbin

Model-free functional MRI analysis based on unsupervised clustering

Axel Wismüller,[a,b] Anke Meyer-Bäse,[b,*] Oliver Lange,[b] Dorothee Auer,[c] Maximilian F. Reiser,[a] and DeWitt Sumners[d]

[a] *Department of Clinical Radiology, Ludwig-Maximilians University, Munich 80336, Germany*
[b] *Department of Electrical and Computer Engineering, Florida State University, Tallahassee, FL 32310-6046, USA*
[c] *Max Planck Institute of Psychiatry, Munich 80804, Germany*
[d] *Department of Mathematics, Florida State University, Tallahassee, FL 32306-4510, USA*

Received 11 March 2003

Abstract

Conventional model-based or statistical analysis methods for functional MRI (fMRI) are easy to implement, and are effective in analyzing data with simple paradigms. However, they are not applicable in situations in which patterns of neural response are complicated and when fMRI response is unknown. In this paper the ''neural gas'' network is adapted and rigourosly studied for analyzing fMRI data. The algorithm supports spatial connectivity aiding in the identification of activation sites in functional brain imaging. A comparison of this new method with Kohonen's self-organizing map and with a fuzzy clustering scheme based on deterministic annealing is done in a systematic fMRI study showing comparative quantitative evaluations. The most important findings in this paper are: (1) both ''neural gas'' and the fuzzy clustering technique outperform Kohonen's map in terms of identifying signal components with high correlation to the fMRI stimulus, (2) the ''neural gas'' outperforms the two other methods with respect to the quantization error, and (3) Kohonen's map outperforms the two other methods in terms of computational expense. The applicability of the new algorithm is demonstrated on experimental data.

Keywords: Fuzzy clustering; ''Neural gas'' network; Self-organizing map; fMRI

1. Introduction

Functional magnetic resonance imaging with high temporal and spatial resolution represents a powerful technique for visualizing rapid and fine activation patterns of the human brain [4,8,10,11,17]. As is known from both theoretical estimations and experimental results [1,10,16], an activated signal variation appears very low on a clinical scanner. This motivates the application of analysis methods to determine the response waveforms and associated activated regions. Generally, these techniques can be divided into two groups: Model-based techniques require prior knowledge about activation patterns, whereas model-free techniques do not. However, model-based analysis methods impose some limitations on data analysis under complicated experimental conditions. Therefore, analysis methods that do not rely on any assumed model of functional response are considered more powerful and relevant. There are two kinds of model-free methods. The first method, principal component analysis (PCA) [2,19] or independent component analysis (ICA) [13,14], transforms original data into high-dimensional vector space to separate functional response and various noise sources from each other.

The second method, fuzzy clustering analysis [3,5,20,22] or self-organizing map [6,15,22], attempts to classify time signals of the brain into several patterns according to temporal similarity among these signals.

In this paper, we propose to employ the ''neural gas'' network to increase the analysis power without sacrifying efficiency. In a systematic manner, we will compare and evaluate the results obtained based on this new approach with the traditional Kohonen's self-organizing map (SOM) and with the fuzzy clustering scheme based on deterministic annealing [18,22]. In this context, we put special emphasis on the methodology rather than the imaging application.

* Corresponding author. Fax: 1-850-410-6479.
E-mail address: amb@eng.fsu.edu (A. Meyer-Bäse).

1532-0464/$ - see front matter © 2004 Elsevier Inc. All rights reserved.
doi:10.1016/j.jbi.2003.12.002

2. The clustering algorithms

Functional organization of the brain is based on two complementary principles, localization and connectionism. Localization means that each cognitive function is performed mainly by a small set of the cortex. Connectionism, on the other hand, expresses that the brain regions involved in a certain visual cortex function are widely distributed, and thus the brain activity necessary to perform a given task may be the functional integration of activity in distinct brain systems. It is important to stress that in neurobiology the term "connectionism" is used in a different sense than that used in the neural network terminology.

The following sections are dedicated to presenting the algorithms and evaluate the discriminatory power of unsupervised clustering techniques such as "neural gas" network, fuzzy clustering based on deterministic annealing and Kohonen's self-organizing map. These techniques are based on grouping image pixels together based on the similarity of their intensity profile in time (i.e., their time-courses).

Let n denote the number of subsequent scans in a fMRI study, and let K be the number of pixels in each scan. The dynamics of each pixel $\mu \in \{1,\ldots,K\}$, i.e., the sequence of signal values $\{\mathbf{x}^{\mu}(1),\ldots,\mathbf{x}^{\mu}(n)\}$ can be interpreted as a vector $\mathbf{x}^{\mu}(i) \in \mathbf{R}^n$ in the n-dimensional feature space of possible signal time-series at each pixel (Pixel Time Course, PTC).

Cluster analysis groups image pixels together based on the similarity of their intensity profile in time. In the clustering process, a time course with n points is represented by one point in an n-dimensional Euclidean space which is subsequently partitioned into clusters based on the proximity of the input data.

Here, we employ several vector quantization (VQ) approaches as a method for unsupervised image time-series analysis. VQ clustering identifies several groups of pixels with similar PTC, while these groups or clusters are represented by prototypical time-series called codebook vectors (CV) located at the center of the corresponding clusters. The CVs represent prototypical PTCs sharing similar temporal characteristics. Thus, each PTC can be assigned in the crisp clustering scheme to a specific CV according to a minimal distance criterion, while in the fuzzy scheme according to a membership to several CVs. Accordingly, the outcomes of VQ approaches for fMRI data analysis can be plotted as "crisp" or "fuzzy" cluster assignment maps.

VQ approaches determine the cluster centers $\mathbf{w}_i$ by an iterative adaptive update based on the following equation:

$$\mathbf{w}_i(t+1) = \mathbf{w}_i(t) + \epsilon(t) a_i(\mathbf{x}(t), C(t), \kappa)(\mathbf{x}(t) - \mathbf{w}_i(t)), \tag{1}$$

where $\epsilon(t)$ represents the learning parameter, a_i a codebook $C(t)$ dependent cooperativity function, κ a cooperativity parameter, and $\mathbf{x}$ a randomly chosen feature vector. For fMRI, the feature vector represents the PTC.

2.1. Kohonen's self-organizing map

Kohonen's self-organizing map generates nodes on a two-dimensional lattice in which the distribution of these nodes corresponds to the proximity of their associated node patterns in the signal intensity space. The benefits of this clustering technique are: (1) if started with an adequate number of neurons, it can find distinctive features in the data even if they are less predominant, and (2) the emerging node patterns are ordered according to their proximity properties in the data space. This topology-preserving technique enables the forming of superclusters by fusing nodes, and thus provides a way to visualize high-dimensional data sets. Its advantages in analyzing fMRI data were demonstrated in [6].

The learning rule for the Kohonen's self-organizing map is given below

$$\mathbf{w}_i(t+1) = \mathbf{w}_i(t) + \epsilon(t) \exp\left(-\frac{d_{ij}}{\sigma^2}\right)(\mathbf{x}(t) - \mathbf{w}_i(t)), \tag{2}$$

where d_{ij} is a distance between neurons i and j determined by a neighborhood relation and σ^2 is an operating parameter. $\exp(-(d_{ij}/\sigma^2))$ takes the maximum value of one for $i = j$, namely for the firing neuron, and decreases when the distance becomes large.

2.2. Fuzzy clustering based on deterministic annealing

Another proven tool for the analysis of fMRI time-series is given by a fuzzy clustering technique based on deterministic annealing [18,22].

The learning rule for fuzzy clustering based on deterministic annealing is given below

$$\mathbf{w}_i(t+1) = \mathbf{w}_i(t) + \epsilon(t) \frac{\exp -||\mathbf{x}(t) - \mathbf{w}_i(t)||^2/2\rho^2}{\sum_i \exp -||\mathbf{x}(t) - \mathbf{w}_i(t)||^2/2\rho^2} \times (\mathbf{x}(t) - \mathbf{w}_i(t)), \tag{3}$$

where ρ is the "fuzzy range" of the model, and defines a length scale in data space and is annealed to repeatedly smaller values in the VQ approach. In parlance of statistical mechanics, ρ represents the temperature T of a multiparticle system by $T = 2\rho^2$.

The cooperativity function

$$a_i = \frac{\exp -||\mathbf{x}(t) - \mathbf{w}_i(t)||^2/2\rho^2}{\sum_i \exp -||\mathbf{x}(t) - \mathbf{w}_i(t)||^2/2\rho^2}$$

is the so-called *softmax* activation function, and accordingly the outputs lie in the interval [0,1] and they

sum up to one. In deterministic annealing some form of randomness is incorporated into the energy function itself, which is then deterministically optimized at a sequence of decreasing temperatures [18]. The algorithm starts with one cluster representing the center of the whole data set. Gradually, the large clusters split up into smaller ones representing smaller regions in the feature space. This represents a major advantage over fuzzy c-means clustering since this algorithm does not employ prespecified cluster centers.

This clustering procedure identifies groups of pixels sharing similar properties of signal dynamics, and thus enables the interpretation of the physiological part of the experiment. The main differences between SOM and minimal free energy vector quantization were pointed out in [22]: (1) the hierarchical and multiresolution aspect of data analysis, (2) monitoring based on different control parameters (free energy, entropy) facilitates straightforward cluster splitting, and (3) the learning rule based on a stochastic gradient descent on an explicitely given error function.

2.3. "Neural gas" network

The "neural-gas" algorithm [12] is an efficient approach which, applied to the task of vector quantization, (1) converges quickly to low distortion errors, (2) reaches a distortion error[1] lower than that from Kohonen's feature map, and (3) at the same time obeys a gradient descent on an energy surface.

Instead of using the distance $||\mathbf{x} - \mathbf{w_i}||$ or of using the arrangement of the $||\mathbf{w_i}||$ within an external lattice, it utilizes a neighborhood-ranking of the reference vectors $\mathbf{w_i}$ for the given data vector $\mathbf{x}$.

The learning rule for the "neural gas" network is given below

$$\mathbf{w}_i(t+1) = \mathbf{w}_i(t) + \epsilon(t)\exp\{-k_i(\mathbf{x}, \mathbf{w_i}/\lambda)\}(\mathbf{x}(t) - \mathbf{w}_i(t)), \tag{4}$$

where $k_i = 0, \ldots, N-1$ represents the rank index describing the "neighborhood-ranking" of the reference vectors $\mathbf{w_i}$ to the data vector $\mathbf{x}$ in a decreasing order, N is the number of units in the network, and λ determines the number of neural units changing their synapses with every iteration. The step size $\epsilon \in [0,1]$ describes the overall extent of the modification.

Martinetz et al. [12] showed that the average change of the reference vectors corresponds to an overdamped motion of particles in a potential that is given by the negative data point density. Superimposed on the gradient of this potential is a "force," which points toward the direction of the space where the particle density is low. This "force" is the result of a repulsive coupling between the particles (reference vectors). In its form it resembles an entropic force and tends to homogeneously distribute the particles (reference vectors) over the input space, like the case of a diffusing gas. This suggests the name for the "neural-gas" algorithm. It is interesting also to mention that the reference vectors $\mathbf{w_i}$ change their locations slowly but permanently and, $\mathbf{w_i}$ that are neighboring at an early stage of the adaptation procedure might not be neighboring anymore at a more advanced stage.

Another important feature of the presented algorithm compared to Kohonen algorithm is that it does not require a prespecified graph (network). In addition, it can produce topologically preserving maps, which is only possible if the topological structure of the graph matches the topological structure of the data manifold. In cases, however, where it is not possible to a priori determine an appropriate graph, for example, in cases where the topological structure of the data manifold is not known a priori or is too complicated to be specified, Kohonen's algorithm necessarily fails in providing perfectly topology preserving maps. The "neural-gas" algorithm enables data analysis without knowledge of the stimulation paradigm [9].

3. Results and discussion

FMRI data were recorded from five subjects (3 female, 2 male, age 20–37) performing a visual task. In all five subjects, five slices with 100 images (TR/TE = 3000/60 ms) were acquired with five periods of rest and five photic simulation periods starting with rest. Simulation and rest periods comprised 10 repetitions each, i.e., 30 s. Resolution was $3 \times 3 \times 4$ mm. The slices were oriented parallel to the calcarine fissure. Photic stimulation was performed using an 8 Hz alternating checkerboard stimulus with a central fixation point and a dark background with a central fixation point during the control periods [22]. The first scans were discarded for remaining saturation effects [7]. Motion artifacts were compensated by automatic image alignment (AIR, [21]).

The clustering results were evaluated by (1) assessment of cluster assignment maps, (2) task-related activation maps, and (3) associated time-courses. Cluster assignment maps represent cluster membership maps obtained based on a minimal distance criterion in the pixel time course space. For the fMRI data, a comparative quantitative evaluation among the three clustering techniques, SOM, "neural gas" network, and fuzzy clustering (FC) based on deterministic annealing, was performed.

3.1. Estimation of the clustering model

To decide to what extent clustering techniques of fMRI time-series depend on the employed algorithm, we

[1] This error measures the fidelity of data encoding, and is given by the squared Euclidean distance between the data vectors and the corresponding approximating reference vectors.

first have to look at the optimal number of codebook vectors determined by each algorithm.

Therefore, it is significant to find a fixed number of CVs that can theoretically predict new observations under same conditions. To do so, we compared the three proposed algorithms for 8, 16, and 36 CVs in terms of: (1) the component time course most closely matching the visual task reference function which is found by each of the three techniques, (2) the normalized quantization error, and (3) the necessary simulation time.

The obtained results are plotted in Fig. 1. In the following we will give the set of parameters. For SOM we chose: (1) an one-dimensional lattice, and (2) the maximal number of iterations equals 1000. For "neural gas" network we choose: (1) the learning parameters $\epsilon_i = 0.5$ and $\epsilon_f = 0.005$, and (2) the lattice parameters λ_i equals half the number of classes and $\lambda_f = 0.01$, and (3) the maximal number of iterations equals 1000. And last, for fuzzy clustering based on deterministic annealing we set: (1) neurons' initialization with principal components, (2) learning parameter $\rho_{final} = 0.01$ and updating based on a linear annealing scheme, and (3) the maximal number of iterations equals 100.

From Fig. 1 we see that the lowest quantization error is achieved by the "neural gas" network, which at the same time provides the best correlation for eight CVs. In this situation, it also outperforms the fuzzy clustering based on deterministic annealing.

The clustering results for the new method, the "neural gas" network, are shown in Figs. 2 and 3. Fig. 2 illustrates the so-called assignment maps where all the pixels belonging to a specific cluster are highlighted. The assignment between a pixel and a specific cluster is given by the minimum distance between the PTC and the CV from the established codebook. On the other hand, each CV shown in Fig. 3 can be viewed as the cluster-specific weighted average of all pixel time-courses. The first two codebook vectors in Fig. 3 are similar to the stimulus function. Their corresponding cluster assignment maps in Fig. 2 can be attributed to activation of the visual cortex.

3.2. Characterization of task-related effects

For all subjects, and runs, cluster assignment maps, unique task-related activation maps and associated time-courses were obtained by all three clustering techniques.

Fig. 4 shows for 36 CVs the component time course most closely associated with the visual task for all three clustering techniques. This time course can serve as an estimate of the stimulus reference function used in the fMRI experiment, as identified by the specific clustering technique. The best results are achieved by the "neural gas" network and the fuzzy clustering based on deterministic annealing, yielding almost identical estimated reference functions, and a correlation coefficient of $r = 0.9984$ between those two. This striking similarity

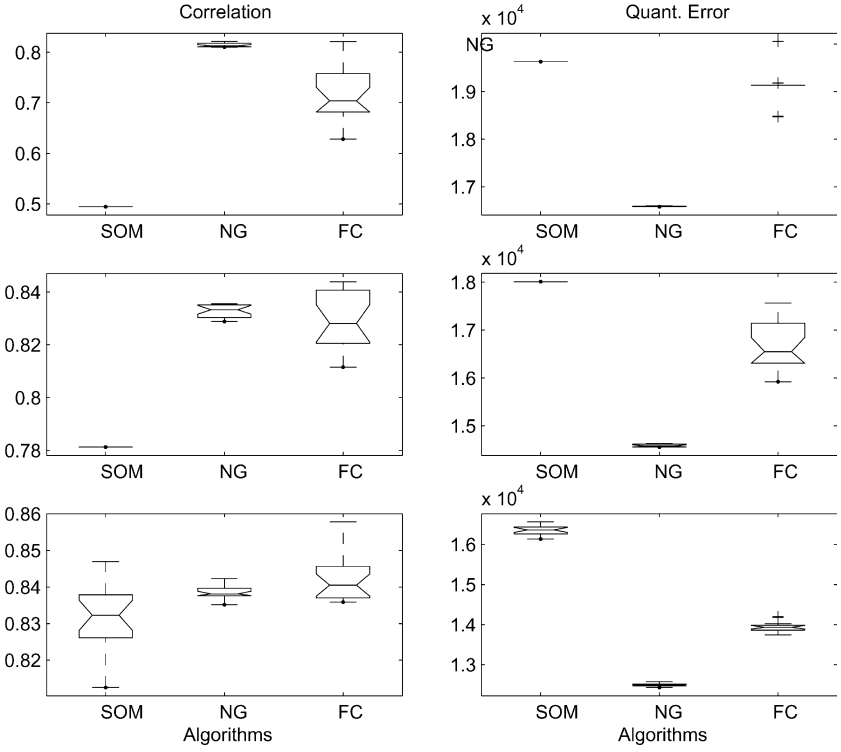

Fig. 1. Results of the three clustering techniques obtained for different numbers of codebook vectors, considering 20 runs each. From top to bottom, the results for 8, 16, and 36 CVs are visualized. The plots show the best correlation coefficients between the found consistently task-related (CTR) components to the given task reference function, and the corresponding quantization error per voxel.

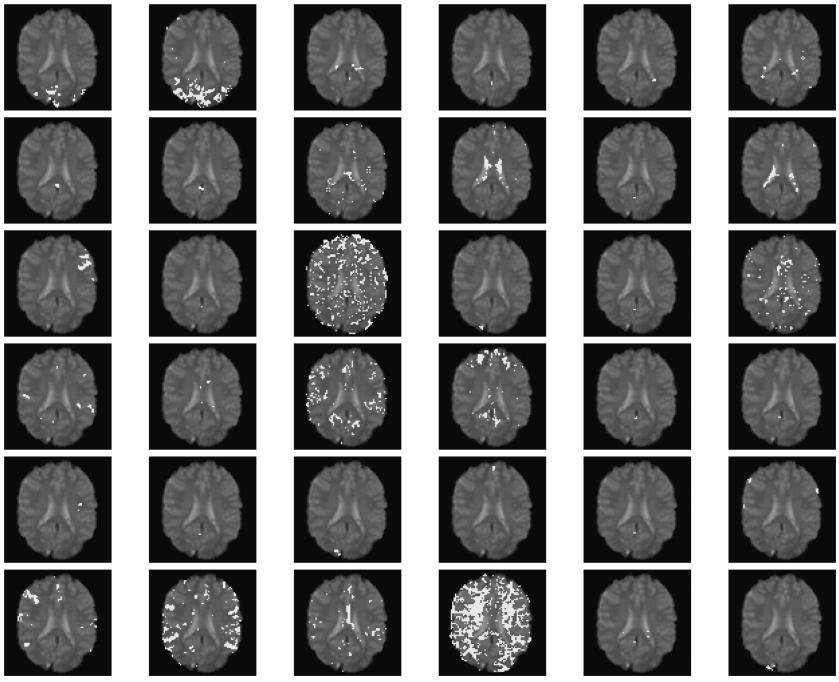

Fig. 2. Cluster assignment maps for cluster analysis based on the "neural gas" network of a visual stimulation fMRI experiment obtained for 36 CVs.

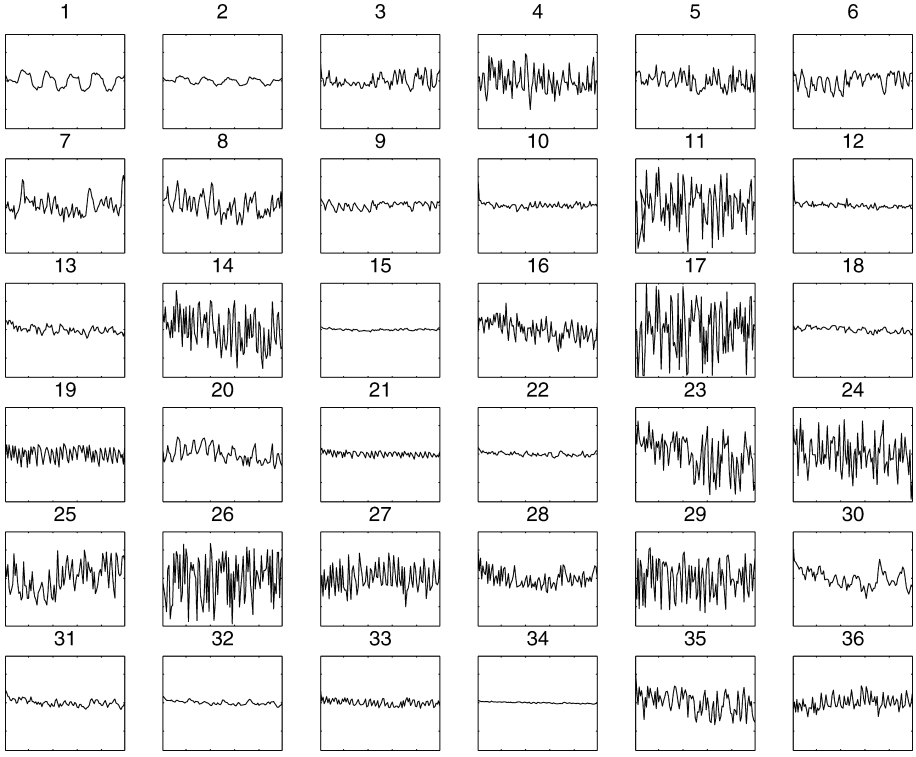

Fig. 3. Associated codebook vectors for the "neural gas" network clustering as shown in Fig. 2. Assignment of the codebook vectors corresponds to the order of the assignment maps shown in Fig. 2.

between these neural networks is also visualized in Fig. 5 which shows the activation maps as a comparison of results obtained by the three techniques.

The results found in Fig. 5 motivate a closer look at the activation maps of each technique such that a more general statement regarding the differentiation

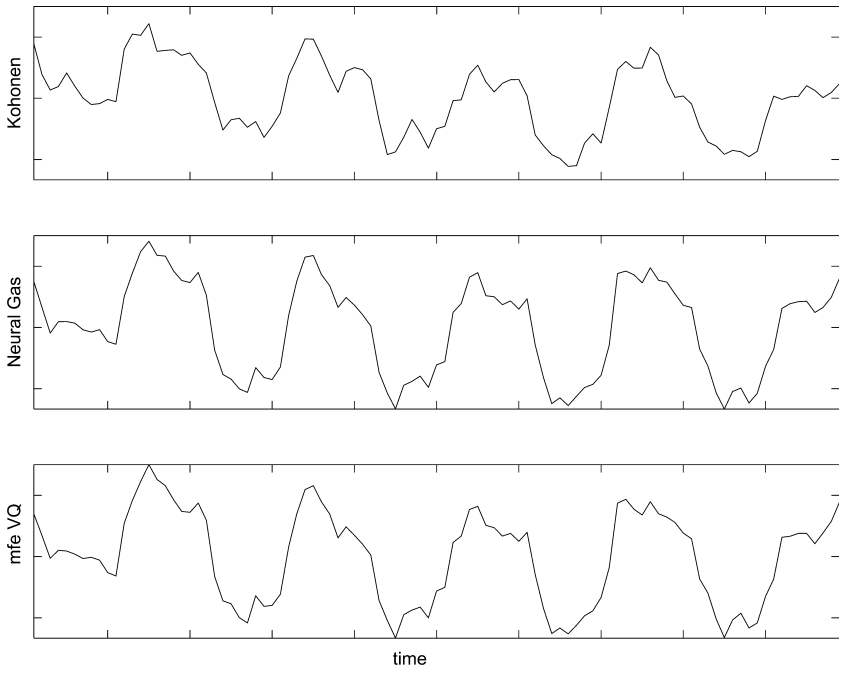

Fig. 4. Computed estimates of the reference functions for the three techniques, SOM, "neural gas" network, and FC, for 36 codebook vectors. The found correlation coefficients are: $r = 0.8394$ for SOM, $r = 0.8416$ for "neural gas" network, and $r = 0.8408$ for FC.

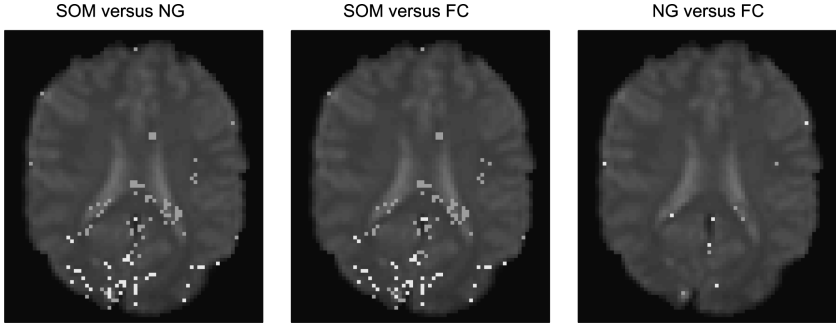

Fig. 5. Comparison of the results for the three techniques, SOM, "neural gas" network, and FC for 16 codebook vectors. The shown activation maps show only the pairwise differences for 16 codebook vectors. The darker pixels show active voxels for the first technique, while the lighter pixels show the active voxels for the second technique.

capabilities of each technique is possible. Two representation modalities are chosen: one based on the so-called z-statistics [13], and the other based on the correlation value. Fig. 6 shows the activation maps for each of the three techniques based on the z-statistics. The z score for a map value, indicates how far and in

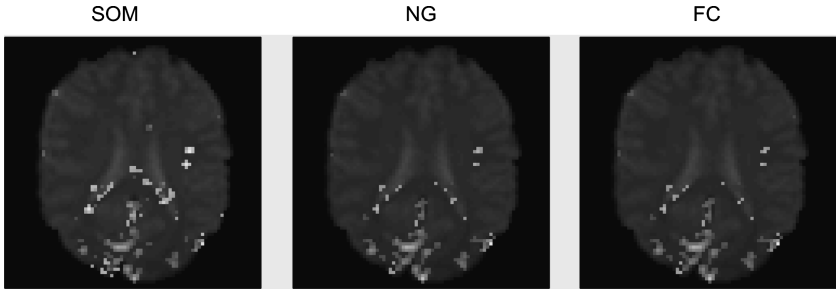

Fig. 6. Activation z-maps for the three techniques, SOM, "neural gas" network, and FC for 16 codebook vectors. The threshold for an active pixel was set at $|z| > 2$.

what direction, that value deviates from its distribution's mean, expressed in units of its distribution's standard deviation. The mathematics of the z score transformation are such that if every value in a distribution is converted to its z score, the transformed scores will necessarily have a mean of zero and a standard deviation of one.

Z scores are sometimes called "standard scores." The z score transformation is especially useful when seeking to compare the relative standings of values from distributions with different means and/or different standard deviations. Z scores are especially informative when the distribution to which they refer is normal. In every normal distribution, the distance between the mean and a given z score cuts off a fixed proportion of the total area under the curve.

The lighter a pixel is, the more correlated is the corresponding pixel to the CTR. The "neural gas" network and the FC activation maps appear very similar to each other.

The activation maps obtained based on the correlation analysis show consistent results with those based on z-statistics. Interestingly, the results obtained by the "neural gas" network and the FC based on z-statistics are similar as shown in Fig. 7.

3.3. Exploratory analysis of ancillary findings

From Figs. 2 and 3, we can also obtain some insight in the type of artifactual components. For the cluster assignment maps in Fig. 3, cluster 13 and 31 may be assigned to a co-activation of the frontal eye fields induced by stimulus onset. There may be some type of physiological relatedness between cluster 13 and 31 on one hand, and between cluster 1 and 2 showing high correlation with the stimulus function, on the other hand. However, this connection is not revealed by the feature space metric, and thus is not supported by clustering approaches based on this metric. Fig. 8 for example shows the codebook vector and the assignment map for a cluster indicative of left-handed frontal eye-field co-activation.

An additional benefit from unsupervised clustering techniques represents the ability to identify data highly indicative of artifacts, e.g., ventricular pulsation or through plane motion. Fig. 9 for example shows the region of the inner ventricles. It is important to mention that these effects could not have been detected by model-based approaches.

An important aspect in real-time analysis is the required processing time associated with each technique.

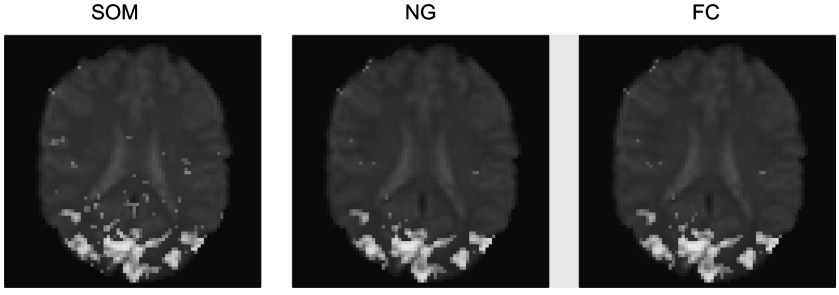

Fig. 7. Activation maps based on correlation for the three techniques, SOM, "neural gas" network, and FC. A voxel is considered active by correlation if $r \geqslant 0.47$. The maximal correlation coefficient r obtained by each of the three techniques is: 0.72 (SOM), 0.83 (NG), and 0.82 (FC).

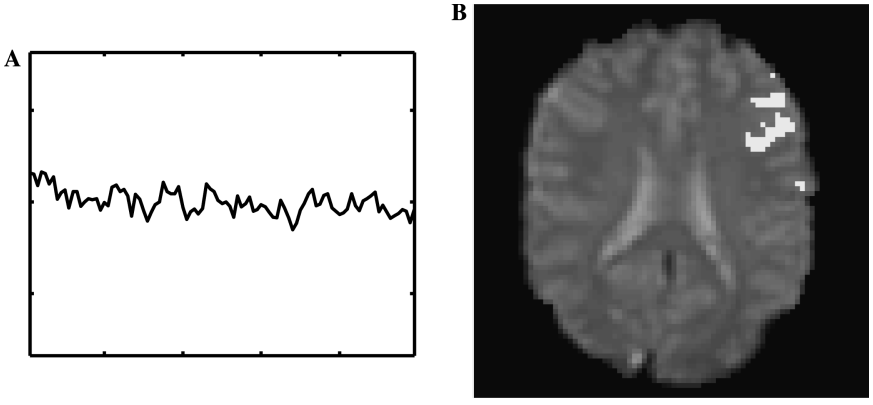

Fig. 8. Cluster indicative of a co-activation of the left frontal eye field induced by stimulus onset obtained from a visual stimulation experiment. (A) Cluster assignment map, (B) codebook vector.

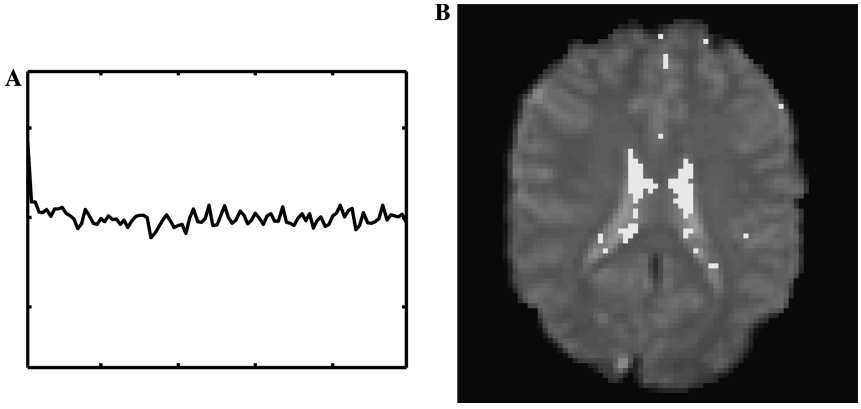

Fig. 9. Cluster representing the region of the inner ventricles obtained from a visual stimulation experiment. (A) Cluster assignment map, (B) codebook vector.

Table 1
Simulation time aspects for clustering techniques in function of the number of codebook vectors

	$N = 8$	$N = 16$	$N = 36$
Kohonen's map	3.77	5.09	6.70
"Neural gas" network	11.80	13.66	20.89
Fuzzy clustering	96.61	278.82	629.71

Time is given in seconds.

A comparison between these techniques is given in Table 1. For the same number of target components, the fastest technique is the Kohonen map.

4. Conclusion

In the present paper, we have experimentally compared two proven clustering algorithms, the SOM and the fuzzy clustering based on deterministic annealing, with a novel and powerful algorithm, the "neural gas" network. The goal of the paper was to demonstrate that unsupervised clustering techniques represent a useful strategy for the analysis of time-courses from fMRI data sets. The clustering results proved to reveal extremely well the structure of the data set.

It has been shown that both "neural gas" network and fuzzy clustering based on deterministic annealing outperform the SOM in terms of found component time course, quantization error, and activation maps, when applied to fMRI studies. However, SOM turned out to be the fastest algorithm, while the "neural gas" network proved to be an adequate clustering technique for the identification of signal components with high correlation to the stimulus function. All unsupervised clustering techniques can be employed to identify interesting ancillary findings that cannot be detected by model-based approaches. The applicability of the new algorithm is demonstrated on experimental data. We conjencture that the method can serve as a multipurpose computer vision strategy to image-time series analysis and visualization for many fields ranging from biomedical basic research to clinical assessment of patient data. In particular, beyond the application to fMRI data analysis discussed in this paper, the method exhibits a specific potential to serve in applications refering to dynamic contrast-enhanced perfusion MRI for the diagnosis of cerebrovascular disease or magnetic resonance mammography for the analysis of suspicious lesions in patients with breast cancer.

Acknowledgment

The authors greatly appreciate the programming efforts of Thomas Dan Otto.

References

[1] Boxerman J, Bandettini P, Kwong K, Baker J. The intravascular contribution to fmri signal change: Monte Carlo modeling and diffusion-weighted studies in vivo. Magn Reson Med 1995;34(8):4–10.
[2] Backfrieder W, Baumgartner R, Samal M, Moser E, Bergmann H. Quantification of intensity variations in functional mr images using rotated principal components. Phys Med Biol 1996;41(8):1425–38.
[3] Baumgartner R, Ryder L, Richter W, Summers R, Jarmasz M, Somorjai R. Comparison of two exploratory data analysis methods for fmri: fuzzy clustering versus principal component analysis. Magn Reson Imaging 2000;18(8):89–94.
[4] Bandettini P, Wong E, Hinks R, Tikofski R, Hyde J. Time course epi of human brain function during task activation. Magn Reson Med 1992;25(8):390–7.
[5] Chuang K, Chiu M, Lin C, Chen J. Model-free functional mri analysis using kohonen clustering neural network and fuzzy c-means. IEEE Trans Med Imaging 1999;18(8):1117–28.
[6] Fisher H, Hennig J, Clustering of functional mr data. In: Proceedings ISMRM 4rd Annual Meeting 1996;96(8):1179–83.
[7] Friston K, Jezzard P, Turner R. Analysis of functional mri time-series. Hum Brain Mapp 1994;1(8):153–71.

[8] Frahm J, Merboldt K, Hanicke W. Functional mri of human brain activation at high spatial resolution. Magn Reson Med 1992;29(8):139–44.
[9] Frisone F, Vitali P, Rodriguez G, Pilot A, Nobili F, Sardanelli F, Rosa M. Self-organizing neural networks for fmri signal detection. 5th International Conference on Functional Mapping of the Human Brain Poster No. 63, 5, 1999.
[10] Kwong K, Belliveau J, Chesler D. Dynamic magnetic resonance imaging of human brain activity during primary sensor stimulation. Proc Natl Acad Sci USA 1992;89(8):5675–9.
[11] Kwong K. Functional magnetic resonance imaging with echo planar imaging. Magn Reson Q 1992;11(8):1–20.
[12] Martinetz T, Berkovich S, Schulten K. Neural gas network for vector quantization and its application to time-series prediction. IEEE Trans Neural Netw 1993;4(4):558–69.
[13] McKeown M, Jung T, Makeig S, Brown G, Jung T, Kindermann S, Bell A, Sejnowski T. Analysis of fmri data by blind separation into independent spatial components. Hum Brain Mapp 1998;6(8):160–88.
[14] McKeown M, Jung T, Makeig S, Brown G, Jung T, Kindermann S, Bell A, Sejnowski T. Spatially independent activity patterns in functional magnetic resonance imaging data during the stroop color-naming task. Proc Natl Acad Sci USA 1998;95(8):803–10.
[15] Ngan S, Hu X. Analysis of fmri imaging data using self-organizing mapping with spatial connectivity. Magn Reson Med 1999;41(8):939–46.
[16] Ogawa S, Lee T, Barrere B. The sensitivity of magnetic resonance image signals of a rat brain to changes in the cerebral venous blood oxygenation activation. Magn Reson Med 1993;29(8):205–10.
[17] Ogawa S, Tank D, Menon R. Intrinsic signal changes accompanying sensory stimulation: functional brain mapping with magnetic resonance imaging. Proc Natl Acad Sci USA 1992;89(8):5951–5.
[18] Rose K, Gurewitz E, Fox G. Vector quantization by deterministic annealing. IEEE Trans Inf Theory 1992;38(3):1249–57.
[19] Sychra J, Bandettini P, Bhattacharya N, Lin Q. Synthetic images by subspace transforms i. principal components images and related filters. Med Phys 1994;21(8):193–201.
[20] Scarth G, McIntrye M, Wowk B, Samorjai R. Detection novelty in functional imaging using fuzzy clustering. In: Proceedings SMR 3rd Annual Meeting 1995;95(8):238–42.
[21] Woods R, Cherry S, Mazziotta J. Rapid automated algorithm for aligning and reslicing pet images. J Comput Assist Tomogr 1992;16(8):620–33.
[22] Wismüller A, Lange O, Dersch D, Leinsinger G, Hahn K, Pütz B, Auer D. Cluster analysis of biomedical image time-series. Int J Comput Vision 2002;46(2):102–28.